RSC Advances

PAPER

Cite this: *RSC Adv.*, 2015, **5**, 99008

Amine-functionalized metal organic framework (NH_2-MIL-125(Ti)) incorporated sodium alginate mixed matrix membranes for dehydration of acetic acid by pervaporation

Zhenbo Su,[a] Jian Hua Chen,*[ab] Xue Sun,[a] Yihong Huang[a] and Xinfei Dong[a]

In the present paper, amine-functionalized metal organic framework (NH_2-MIL-125(Ti)) crystal nanoparticles were synthesized and incorporated into a sodium alginate (NaAlg) matrix to prepare novel NH_2-MIL-125(Ti)/NaAlg mixed matrix membranes (MMMs). The prepared NH_2-MIL-125(Ti) crystal nanoparticles and NH_2-MIL-125(Ti)/NaAlg MMMs were characterized by the Fourier transformed infrared spectrum, X-ray diffraction, atomic force microscopy, transmission electron microscopy and contact angle goniometer. The pervaporation performance of the as-prepared NH_2-MIL-125(Ti)/NaAlg MMMs have been tested and compared with a pristine NaAlg membrane for dehydrating acetic acid. The experimental results indicated that amine-functionalized NH_2-MIL-125(Ti) crystal nanoparticles were confirmed as a promising filler to improve the separation performance of NH_2-MIL-125(Ti)/NaAlg MMMs for water and acetic acid mixtures. Both the flux and selectivity of the NH_2-MIL-125(Ti)/NaAlg MMMs were significantly improved by incorporating 6 wt% of NH_2-MIL-125(Ti) nanoparticles. The pervaporation performances of NH_2-MIL-125(Ti)/NaAlg-6 MMMs were greatly influenced by feed temperature, feed acetic acid concentration and feed flow rate. In a word, the as-prepared NH_2-MIL-125(Ti)/NaAlg MMMs could be considered as potential candidates for practical acetic acid dehydration.

Received 11th October 2015
Accepted 5th November 2015

DOI: 10.1039/c5ra21073a

www.rsc.org/advances

1 Introduction

Acetic acid is an important organic intermediate used in the production of acetic anhydride, vitamins, vinyl acetate, terephthalic acid, cellulose esters and other chemicals.[1–3] Because of the small differences in the volatility between water and acetic acid in high concentration acetic acid solutions, the separation of acetic acid and water mixtures using distillation is an energy intensive process.[4–6] Water and acetic acid mixtures are often encountered in the production of acetic acid itself, vinyl acetic, phthalic anhydride, *etc.*[7] The separation of water and acetic acid is of great importance for the chemical industry. Pervaporation is a novel and promising membrane separation technology with high selectivity, handy implementation, and energy efficiency, especially in separation azeotropic mixtures and close-boiling mixtures.[8,9] From the standpoint of energy-saving, pervaporation appears to be an attractive method for dehydration of acetic acid.

An ideal pervaporation process should has high performance membrane which has superior permeability and selectivity, excellent durability, high mechanical and thermally stability, and economic viability. Polymer-based pervaporation membranes that possess intrinsic advantages such as good film forming ability, good process ability, and low cost, however, which also usually suffer from the compromise of permeability and selectivity, or trade-off effect.[10,11] Therefore, heterogeneous mixed matrix membranes (MMMs) consisting of nanometric inorganic fillers embedded in a polymeric matrix have been proved a feasible approach to overcome the trade-off effect.[12–14] However, MMMs with inorganic fillers often suffer from the incompatibility between the inorganic and organic phases. Metal organic frameworks (MOFs) is a kind of crystalline porous materials that belong to organic–inorganic hybrid compounds. Organic nature of the framework of MOFs may enhance the compatibility between the polymer matrix and the fillers.[15] Meanwhile, MOFs have been confirmed as promising filler material due to their controllable pore size, extra-large surface area, and outstanding adsorption ability.[16] Thus, MMMs with MOFs as fillers have been widely used in gas separation.[17–22] However, only limited studies are for pervaporation process. Liu *et al.* immobilized the organophilic ZIF-8 nanoparticles into poly(methyl-phenyl)siloxane membranes for recovery of bio-butanol *via* pervaporation.[23] They studies indicated a significant improvement in separation performance over the original polymer membrane due to an enhanced adsorption selectivity

[a]*College of Chemistry and Environmental, Minnan Normal University, Zhangzhou, 363000, China. E-mail: jhchen73@126.com; Fax: +86-596-2520035; Tel: +86-596-2591445*

[b]*Fujian Province University Key Laboratory of Modern Analytical Science and Separation Technology, Minnan Normal University, Zhangzhou, 363000, China*

with the incorporation of ZIF-8. Shi *et al.* designed ZIF-8/PBI MMMs by incorporation ZIF-8 nanoparticles into polybenzimidazole membranes for dehydration of alcohols and studied their properties of water permeability and adsorption.[24] Kang *et al.* synthesized ZIF-7/chitosan hybrid membranes for the separation of water/ethanol mixtures, by taking the advantage of strong affinity of chitosan for ZIF-7 nanoparticles.[25] In addition, HKUST-1 was also used as filler in polyimide Matrimids® 5218 membranes for ethanol dehydration.[26] With the addition of this hydrophilic MOFs, the MMMs membranes showed a higher flux without significant changes in the separation factor. Moreover, ZIF-90 was used to fabricate polyimide P84-based MMMs for dehydration of isopropanol.[27] It was found that the flux of the MMMs increased significantly without much decreasing in selectivity in comparison with the corresponding pristine polymers.

Very few works have been done on the titanium-based MOFs materials. Amine-functionalized NH_2-MIL-125(Ti) is one of the titanium-based MOFs that possess a high surface area, and excellent stability in water or organic solvents. Its hydrophilic property has been confirmed by water vapor adsorption.[28–30] Among many organic polymers, sodium alginate (NaAlg) has been widely used in pervaporation dehydration due to its natural occurring hydrophilic biopolymer, even though its main drawback is high swelling in aqueous solution resulting from the presence of lots of carboxyl and hydroxyl groups on the main chains. To overcome these drawbacks, several methods have been tried to improve the effective dehydration performance of the NaAlg-based membranes, which include cross-linking, grafting, blending and composite membranes.[1–4] In the present paper, NH_2-MIL-125(Ti) nanoparticles were incorporated into the NaAlg matrix with the aim of enhancing the separation factor and flux simultaneously. Amine-functionalized NH_2-MIL-125(Ti) nanoparticles containing the $-NH_2$ and –COOH groups on their structure can effectively improve the interfacial bonding between MOFs and the polymer matrix, thereby achieves a uniform dispersion of MOFs into polymer matrix. The separation performance of the NH_2-MIL-125(Ti)/NaAlg MMMs was evaluated by dehydrating of acetic acid.

2. Experiment

2.1. Materials

2-Amino-1,4-benzenedicarboxylic acid (NH_2-BDC) and titanium isopropoxide ($C_{12}H_{28}O_4Ti$) were purchased from Aldrich. Sodium alginate (NaAlg) was purchased from Xilong chemical Co. Ltd. *N*,*N*-Dimethylformamide (DMF), methanol (CH_3OH), and acetic acid (CH_3COOH) were obtained from Shanghai Chemical Reagent Co. Ltd. All of them were used as received and deionized water was used throughout the experiments.

2.2. Synthesis of NH_2-MIL-125(Ti) crystals

The synthesis of highly porous NH_2-MIL-125(Ti) nanoparticles was accomplished using a solvothermal route in a DMF–methanol mixed solvent with NH_2-BDC as the organic linker and titanium isopropoxide as the metal source. In brief, a solution of 3 mmol (0.853 g) of titanium isopropoxide and 6 mmol (1.087 g) of NH_2-BDC in a 50 mL mixture of DMF and methanol (1 : 1, v/v) was prepared and transferred to a 150 mL Teflon-lined autoclave. The Teflon-lined autoclave containing the mixture was placed in an oven and heated at 50 °C for 16 h. After cooling, a yellow powder product was recovered by filtration, washed three times with DMF to remove the unreacted organic ligand, and then washed twice with methanol to exchange DMF. Finally, the obtained yellow solid samples were activated under vacuum at 30 °C for 12 h.

2.3. Membrane preparation

The NH_2-MIL-125(Ti)/NaAlg MMMs were prepared *via* solution casting and solvent evaporation technique. NaAlg (4 g) was dissolved in 80 mL of deionized water by constant stirring at room temperature. Meanwhile, a certain amount of NH_2-MIL-125(Ti) nanoparticles were dispersed in 80 mL of deionized water and sonicated for 30 min. Then, the well dispersed nanoparticles were added into the previously prepared NaAlg solution. Finally, the solution was further stirred for 12 h and kept overnight to release any gases. The obtained homogeneous mixed solution was poured onto a clean glass plate and was heated in an oven at 60 °C for 4 h. Then the dried membrane was peeled off from the glass plate. The loading amount of NH_2-MIL-125(Ti) in the hybrid membrane was defined as:

$$W_{MOF} = \frac{M_{MOF}}{M_{MOF} + M_{NaAlg}} \times 100\% \quad (1)$$

where M_{NaAlg} and M_{MOF} represent the weight of NaAlg and NH_2-MIL-125(Ti), respectively. The weight percents of NH_2-MIL-125(Ti) nanoparticles in the membrane were varied at 0, 3, 6, 10 and 15 wt%, and the membranes were designated as pristine NaAlg membrane, NH_2-MIL-125(Ti)/NaAlg-3, NH_2-MIL-125(Ti)/NaAlg-6, NH_2-MIL-125(Ti)/NaAlg-10 and NH_2-MIL-125(Ti)/NaAlg-15, respectively.

2.4. Characterization of particles and membranes

Crystallographic structure of NH_2-MIL-125(Ti) nanoparticles was investigated using powder X-ray diffraction (XRD, Bruker D8 Advance, Cu Kα radiation). Morphologies of the NH_2-MIL-125(Ti) nanoparticles, pristine NaAlg membrane and NH_2-MIL-125(Ti)/NaAlg-6 were observed with scanning electron microscope (JEOL, JSM-6010LA, Japan). Energy dispersive spectrometry (EDS) elemental mapping was taken using an energy dispersion of X-ray system. The morphology of NH_2-MIL-125(Ti)/NaAlg-6 was also observed with a transmission electron microscope (TEM, FEI Tecnai G20). The Fourier transform infrared spectra (Thermo Scientific Nicolet 8700, USA) of NH_2-MIL-125(Ti) nanoparticles and membranes were obtained with a range of 400–4000 cm^{-1}. To investigate the surface properties of the membrane, the static contact angles between the membranes and water were measured by the pendant drop method using contact angle meter (SL200B, SOLON TECH, Shanghai, China) at room temperature. The atomic force microscopy (CSPM5500, China) was used to observe the

morphological characterization and surface roughness of the prepared membranes, respectively.

2.5. Pervaporation experiments

The pervaporation experiments were conducted on a self-made equipment. Mixtures of acetic acid and water were prepared and hold in a feed tank with a volume capacity of 1 L. The flat membrane was sealed in a stainless steel pervaporation cell. The feed solutions were circulated between the feed tank and the membrane cell. The effective area of membrane sample was 60 cm^2. The downstream side of membrane module was kept about 1 mbar with a vacuum pump. The system was equilibrated for 30 min before the collection of samples. Thereafter, the permeate vapor was collected using a cold trap immersed in liquid nitrogen. The samples were then weighted and the compositions of permeate were analyzed by gas chromatography equipped with a TCD detector. Each sample was analyzed three times and thus the data of flux and composition were achieved by averaged. The permeation flux (J, g m^{-2} h^{-1}) of the membrane is defined as:

$$J = \frac{Q}{A \times t} \tag{2}$$

where Q (g) is the total weight of the permeate, A (m^2) is the effective area of the membrane and t (h) is the permeation time interval for the pervaporation. The separation factor (α) is defined by the equation below:

$$\alpha_{A/B} = \frac{Y_A / Y_B}{X_A / X_B} \tag{3}$$

where X_A, X_B, Y_A and Y_B are the weight fractions of A (water) and B (acetic acid) in the feed and permeate sides, respectively. The separation index (PSI) was calculated by the following equation:

$$\mathrm{PSI} = J(\alpha - 1) \tag{4}$$

Molecular transport of binary liquid mixtures through a dense polymeric membrane in a pervaporation process is generally analyzed by solution-diffusion mechanism, which occurs in three steps: adsorption, diffusion and evaporation. Thus, permeation rate and selectivity are governed by the solubility and diffusivity of each component of the feed. As a result, it is important to estimate the diffusion coefficient of the penetrating molecules to understand the mechanism of molecular transport. From Fick's law of diffusion, the diffusion flux can be expressed as

$$J_i = -D_i \frac{dC_i}{dx} \tag{5}$$

where D_i (m^2 s^{-1}) is the diffusion coefficient, C_i (kg m^{-3}) is the concentration of permeant, and x (m) is the distance from the membrane surface of the feed side. For simplicity, it is assumed that the concentration profile along the diffusion path is linear. And the concentration of component i, C_i, on the membrane surface at the permeate side can be considered to be zero in pervaporation. Applying the boundary conditions ($x = 0$, $C_i = C_0$ and $x = 1$, $C_i = 0$), the diffusion coefficient of component i, D_i, could be calculated as follows

$$D_i = \frac{J_i \delta}{C_0} \tag{6}$$

where δ (m) is the membrane thickness, and C_0 is the concentration of component i on the membrane surface at the feed side.

The experimental flux for each component is calculated as:[31]

$$J_i = J \times y_i \times \frac{m_i}{m_t} \tag{8}$$

where m_i and m_t are the molecular weight of the component i and the mixture, respectively. y_i is the ratio of the molar component concentrations in the permeate. The molar flux for each component j_i (cm^3 (STP) cm^{-2} s^{-1}) is calculated from (ignoring simple conversion terms, m^2 to cm^2, L to cm^3, h to s):[32]

$$j_i = \frac{J_i \times v_i}{m_i} \tag{9}$$

where v_i is the molar volume of gas i (22.4 L (STP) mol^{-1}).

Distribution coefficient (K_i), permeability (P_i) and selectivity ($\alpha_{i,j}$) are denoted by the following equations:[32]

$$k_i = \frac{C_{i,f,m}}{C_{i,f}} \tag{10}$$

$$P_i = D_i \times K_i \tag{11}$$

$$\alpha_{i,j} = \frac{P_i}{P_j} = \frac{D_i}{D_j} \times \frac{K_i}{K_j} = S_d S_k \tag{12}$$

where, $C_{i,f,m}$ and $C_{i,f}$ are liquid concentration in the membrane and on feed side. S_d is relative ability of penetrants to pass through the membrane, and S_k is relative affinity of penetrants to polymer membrane material.

2.6. Membrane swelling study

Swelling experiments were performed in different concentration of acetic acid and water mixtures. The dried membranes were weighed and equilibrated by soaking in acetic acid and water mixtures at 30 °C for 48 h. The swollen membranes were taken out from the bottle, wiped with filter paper to remove the liquid drops on the surface of the membrane samples, and weighed immediately. The same operation was performed at least three times for all the experiments, and the results were averaged. The errors were less than 2.5%. The percentage degree of swelling (DS%) was determined by

$$\mathrm{DS}(\%) = \frac{W_s - W_d}{W_d} \times 100\% \tag{13}$$

where W_s and W_d denote the weights of the swollen membrane and dry membrane, respectively.

3. Results and discussion

3.1. Characterization of NH_2-MIL-125(Ti) crystal nanoparticles and membranes

SEM and TEM were used to study the morphologies of NH_2-MIL-125(Ti) crystal nanoparticles, surface and cross-section of

membranes as well as the particle–polymer interface. Fig. 1a and b show that the NH_2-MIL-125(Ti) crystal nanoparticles display a quasi-cubic tetragonal structure with nanometers size, which is good for fabricating well-formed hybrid membranes. The surface of the pristine NaAlg membrane is dense and defect-free (Fig. 1c and d). SEM images of the surface and cross-section of NH_2-MIL-125(Ti)/NaAlg-6 MMMs, as shown in Fig. 1e and f, indicate that NH_2-MIL-125(Ti) nanoparticles are well dispersed in the polymer matrix without interfacial voids and agglomeration, which is benefit for the selectivity for a pervaporation membrane. The uniform dispersion of NH_2-MIL-125(Ti) crystal nanoparticles in polymer matrix was further verified by EDX mappings of Ti element (Fig. 2).

Fig. 3 shows XRD pattern of the synthesized NH_2-MIL-125(Ti) crystal nanoparticles which is in good agreement with the simulated XRD patterns of NH_2-MIL-125(Ti) reported by the Férey group,[33] indicating a highly crystalline NH_2-MIL-125(Ti) structure. The broad peak in the XRD pattern of pristine membrane indicates its amorphous property. The diffraction patterns of NH_2-MIL-125(Ti) crystal nanoparticles and NH_2-MIL-125(Ti)/NaAlg-6 MMMs match perfectly, suggesting that the structure of NH_2-MIL-125(Ti) crystal nanoparticles was not significantly altered after filling into NaAlg matrix.

For the spectrum of NH_2-MIL-125(Ti) crystal nanoparticles (Fig. 4a), two absorption bands around 1600 and 1500 cm^{-1} were ascribed to carbonyl asymmetric stretching vibrations,

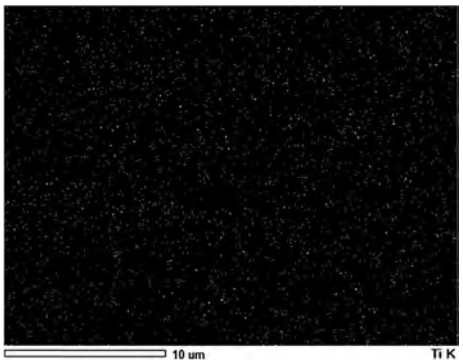

Fig. 2 EDX mapping for Ti of the surface of NH_2-MIL-125(Ti)/NaAlg-6 MMMs.

whereas bands at about 1440 and 1400 cm^{-1} were ascribed to carbonyl symmetric stretching vibrations; the band at 1250 cm^{-1} was attributed the C–H symmetric stretching vibrations of the benzene ring; the bands at about 3500 and 3300 cm^{-1} were due to the stretching vibration of $-NH_2$ group. For the pristine NaAlg membrane and NH_2-MIL-125(Ti)/NaAlg-6 MMMs (Fig. 4b), the bands at 1612 and 1034 cm^{-1} were attributed to the symmetric C=O and asymmetric O–C–O stretching of the carboxyl group, respectively. The bands representing NH_2-MIL-125(Ti) could not be clearly observed on the spectra of the mixed

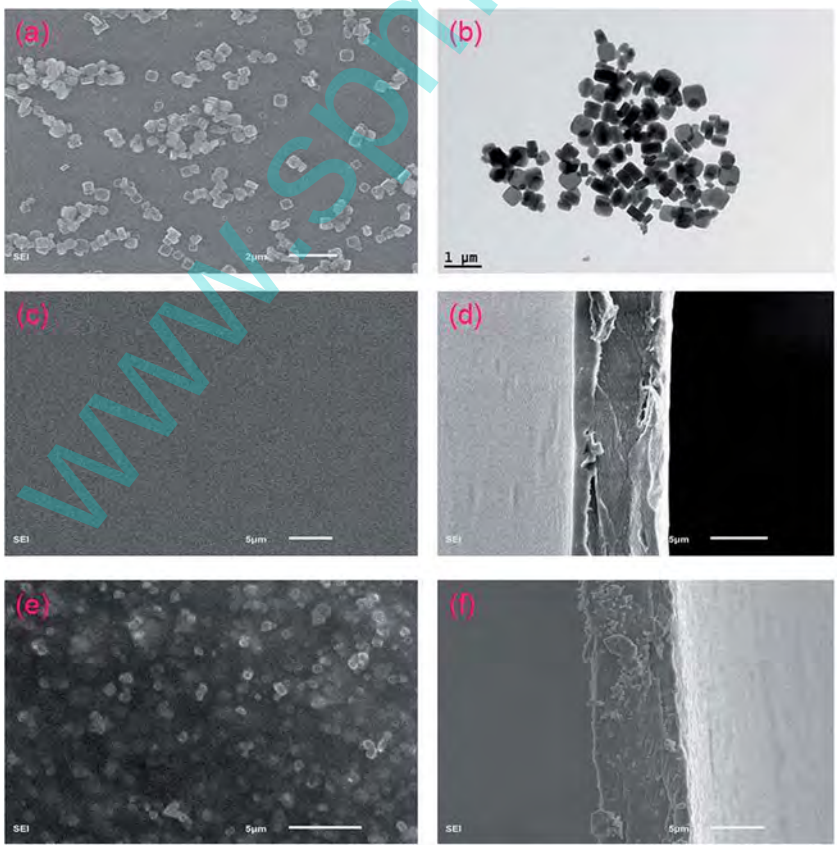

Fig. 1 Images of: (a) NH_2-MIL-125 nanoparticles (SEM); (b) NH_2-MIL-125 nanoparticles (TEM); (c) surface and (d) cross-section of pristine NaAlg membrane (SEM); (e) surface and (f) cross-section of NH_2-MIL-125(Ti)/NaAlg-6 MMMs (SEM).

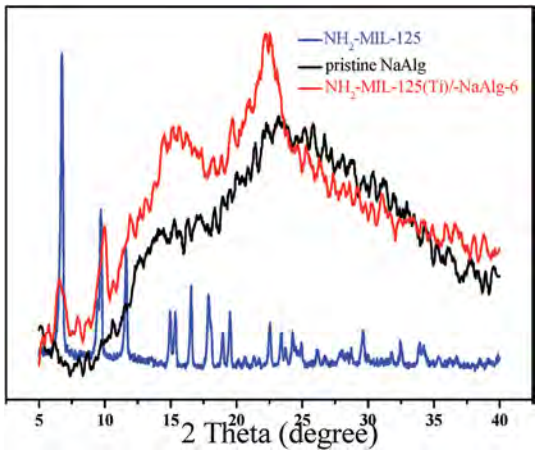

Fig. 3 XRD patterns of the pristine NaAlg membrane, NH_2-MIL-125 nanoparticles and NH_2-MIL-125(Ti)/NaAlg-6 MMMs.

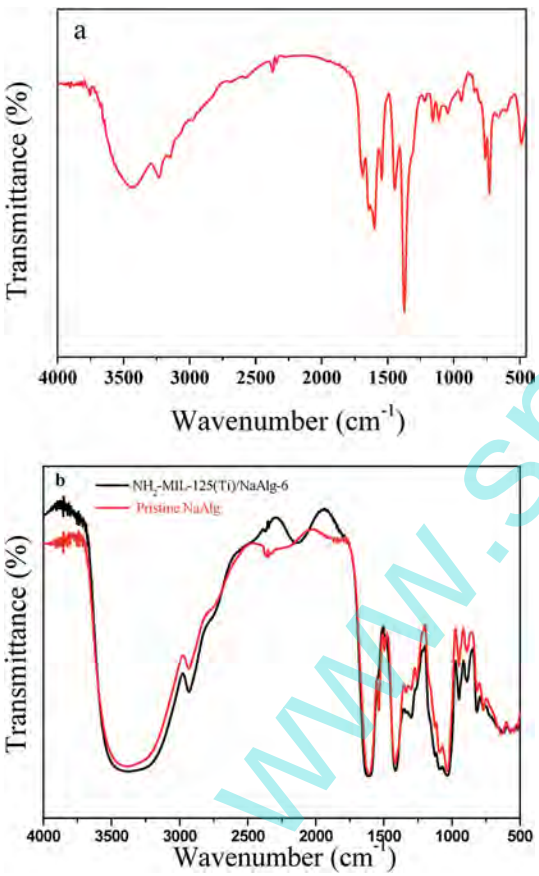

Fig. 4 Infrared spectra of: (a) NH_2-MIL-125 nanoparticles and (b) pristine NaAlg membrane and NH_2-MIL-125(Ti)/NaAlg-6 MMMs.

matrix membrane due to the well dispersed of MOFs nanoparticles in the NaAlg matrix.[34–36]

AFM was also used to assess the changes appeared in surface morphology and roughness of the prepared membranes.[37] Fig. 5 depicts the AFM images of pristine NaAlg membrane and NH_2-MIL-125(Ti)/NaAlg-6 MMMs. A variation in surface morphology and an enhance in surface roughness are observed distinctly when the NH_2-MIL-125(Ti) crystal nanoparticles were incorporated into NaAlg matrix. This indicates an increasing of interface between the feed and NH_2-MIL-125(Ti)/NaAlg-6 MMMs, therefore benefit for permeating molecules adsorbing on the membrane.

The pervaporation performance of a membrane for dehydration of acetic acid is closely related to the hydrophilicity of the separation layer.[38] Generally, the hydrophilicity property of membrane can be assessed by the water contact angle. Smaller the contact angle, stronger hydrophilicity will be for the membrane and *vice versa*. Thus the surface hydrophilicity of the membranes were evaluated by static water contact angle measurement and the results are shown in Fig. 6. The water contact angles of NH_2-MIL-125(Ti) nanoparticles incorporated MMMs are smaller than that of the pristine NaAlg membrane, indicating that the incorporation of NH_2-MIL-125(Ti) nanoparticles enhanced the affinity of the MMMs towards water molecules.

3.2. Swelling of NH_2-MIL-125(Ti)/NaAlg MMMs

In a pervaporation process, membrane swelling plays an important role and affects transport property of permeating molecules.[39] The swelling behaviors of the prepared NH_2-MIL-125(Ti) incorporated MMMs are illustrated in Fig. 7. It shows that the swelling degree of the NH_2-MIL-125(Ti) incorporated MMMs decrease with a decrease of filler concentration and water concentration in feed, which indicates hydrophilic nature of NH_2-MIL-125(Ti)/NaAlg MMMs. As we all known, the swelling degree of the membrane can influence the size of the diffusion channel, therefore, the transport property of permeating molecules.

3.3. Pervaporation performance

3.3.1. Effect of NH_2-MIL-125(Ti) loading amount on MMMs pervaporation performance. Fig. 8 indicates when the NH_2-MIL-125(Ti) loading amount is less than 6 wt%, both water flux and separation factor show conspicuous enhancement with an increase of NH_2-MIL-125(Ti) loading amount in MMMs. This result is attributed to the well dispersed of NH_2-MIL-125(Ti) nanoparticles in NaAlg matrix without interfacial voids and agglomeration, meanwhile, the strong specific interaction between water molecules and the hydrophilic porous NH_2-MIL-125(Ti) nanoparticles also plays an important role. When the NH_2-MIL-125(Ti) loading amount were further increased from 6 wt% to 15 wt%, permeation flux increases significantly while separation factor decreases sharply. The decrease in separation factor is attributed to the formation of voids between the NH_2-MIL-125(Ti) nanoparticles and the polymer matrix resulting from the aggregation of NH_2-MIL-125(Ti) nanoparticles, which become non-selective transport paths for water molecules and acetic acid molecules diffusion through. In order to observe the overall performance of membranes, pervaporation separation index (PSI) were also calculated. As observed in Fig. 9, the prepared MMMs with 6 wt% NH_2-MIL-125(Ti) loading amount exhibits separation factor of 328, flux of 190.7 g m^{-2} h^{-1} and the

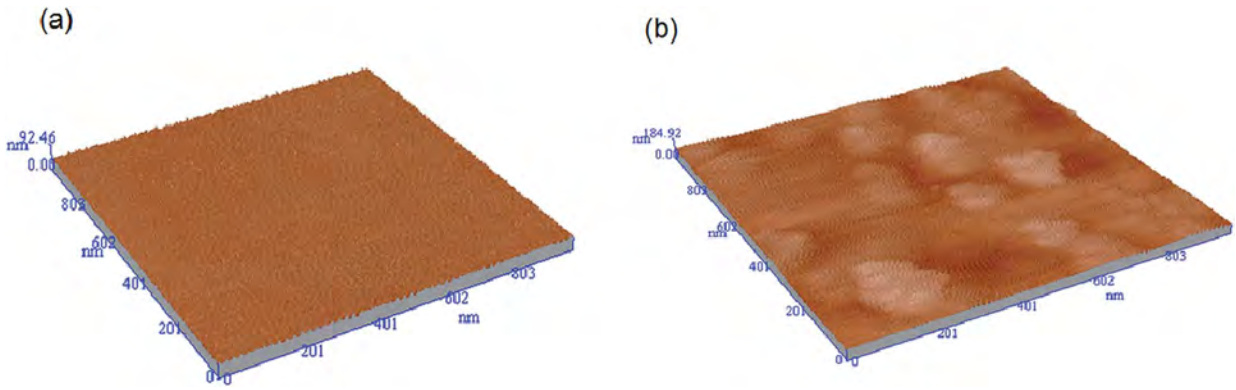

Fig. 5 The AFM images of the fabricated membranes: (a) pristine NaAlg membrane and (b) NH_2-MIL-125(Ti)/NaAlg-6 MMMs.

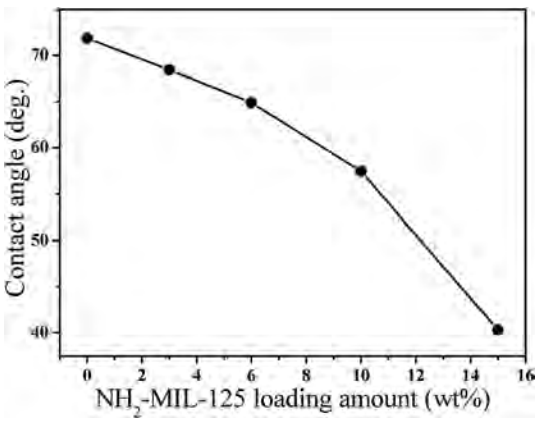

Fig. 6 Effect of NH_2-MIL-125 nanoparticles loading amount on water contact angle.

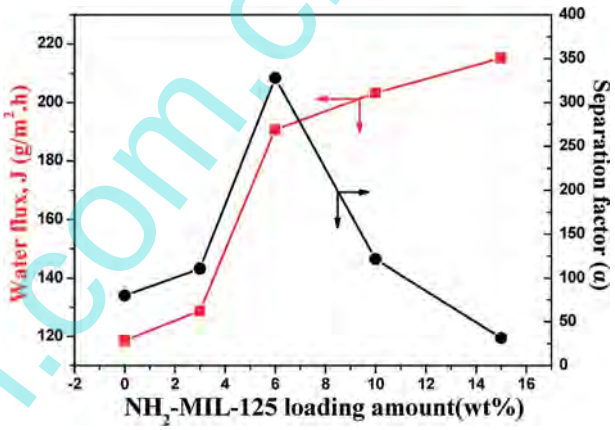

Fig. 8 Effect of NH_2-MIL-125 nanoparticles loading amount on pervaporation performance of NH_2-MIL-125(Ti)/NaAlg MMMs (90 wt% acetic acid in feed at 30 °C).

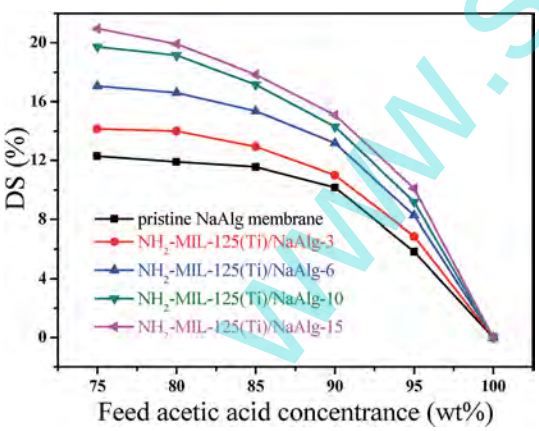

Fig. 7 Swelling degree of pristine NaAlg membrane and NH_2-MIL-125(Ti)/NaAlg MMMs with different NH_2-MIL-125 loading amount at 30 °C.

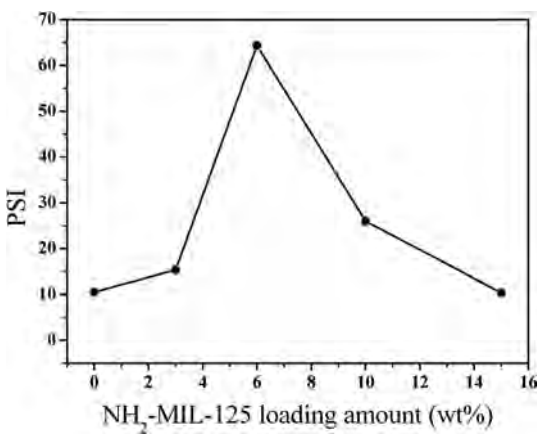

Fig. 9 Effects of NH_2-MIL-125 nanoparticles loading on PSI of NH_2-MIL-125(Ti)/NaAlg MMMs (90 wt% acetic acid in feed at 30 °C).

highest PSI value. As a result, NH_2-MIL-125(Ti)/NaAlg-6 was used for further study.

Water transport through the pristine NaAlg membrane and NH_2-MIL-125(Ti) nanoparticles incorporated NaAlg membranes was investigated by calculating the molar water flux, diffusion coefficient, distribution coefficient, permeability and membrane permselectivity at 90 wt% of acetic acid in the feed at 30 °C. As shown in Table 1, permeability and selectivity of water increase with increasing NH_2-MIL-125(Ti) loading amount up to

Table 1 Molar water flux, water permeability and selectivity values of the membranes at 90 wt% acetic acid in feed at 30 °C

Membranes	Molar water flux, $J_A \times 10^3$ cm^3 (STP) cm^{-2} s^{-1}	Diffusion coefficient, $D_A \times 10^8$ m^2 s^{-1}	Distribution coefficient, K_A	Permeability, $p_A \times 10^9$ m^2 s^{-1}	Selectivity $\alpha_{A,B}$
Pristine NaAlg membrane	1.47	0.48	4.53	2.16	54
NH_2-MIL-125(Ti)/NaAlg-3	1.60	0.51	4.84	2.51	82
NH_2-MIL-125(Ti)/NaAlg-6	2.37	0.76	5.22	3.97	284
NH_2-MIL-125(Ti)/NaAlg-10	2.53	0.78	4.96	2.68	92
NH_2-MIL-125(Ti)/NaAlg-15	2.70	0.81	4.32	2.01	37

6 wt%, but decrease at further increasing of NH_2-MIL-125(Ti) loading amount. Meanwhile, distribution coefficient also gets the maximum value at NH_2-MIL-125(Ti) nanoparticles loading amount of 6 wt%. These can be attributed to the hydrophilicity property of the NH_2-MIL-125(Ti) nanoparticles and moderate swelling degree of the NH_2-MIL-125(Ti)/NaAlg-6 membrane.

3.3.2. Effect of feed temperature on pervaporation performance. Effect of feed temperature on the pervaporation performance of the NH_2-MIL-125(Ti)/NaAlg-6 MMMs for dehydration of acetic acid is revealed in Fig. 10. The water flux increases with an increase of feed temperature, but the selectivity of the membrane based on separation factor decreases significantly. These behaviors can be explained as the following three factors: firstly, the polymer chains become more flexible at a higher temperature, leading to a larger available free volume or diffusion path within the membrane, which reduces the diffusion resistance of the membrane for both acetic acid molecules and water molecules; secondly, as temperature increases, the mass transfer coefficients of the small permeate in the membrane also increase; finally, saturated vapor pressure of the permeate in the upstream side of the membrane increases with an increase in the operating temperature while the pressure at the downstream side of the membrane is hardly affected. Consequently, the increase in vapor pressure difference between the upstream and downstream sides of the membrane enhances the transport driving force.

In addition, the influence of temperature on pervaporation flux can be described through the van't Hoff-Arrhenius equation:[40]

$$J = J_0 \exp(-E_j/RT) \quad (14)$$

where J is the flux, J_0 is the pre-exponential factor, E_p is the activation energy of the pervaporation process, R is the molar gas constant and T is the temperature in Kelvin. The Arrhenius plots of ln J *versus* $1/T$ for the NH_2-MIL-125(Ti)/NaAlg-6 MMMs are linear, as shown in Fig. 11. The activation energy of acetic acid molecules and water molecules are 27.3 and 12.0 kJ mol^{-1}, respectively. Generally, diffusion and permeation of molecules is inversely proportional to the Arrhenius activation energy values.[41] The result exhibits that the activation energy of acetic acid molecules is significantly higher than that of water molecules, indicating that the mass transfer of acetic acid molecules is more sensitive to temperature than water molecules. This further indicates that the as-prepared NH_2-MIL-125(Ti)/NaAlg-6 MMMs is competent for the dehydration of acetic acid.

3.3.3. Effect of acetic acid concentration on pervaporation performance. Effect of acetic acid concentration on the pervaporation performance of the as-prepared NH_2-MIL-125(Ti)/NaAlg-6 MMMs at a given temperature is shown in Fig. 12. It shows that the water flux decreases, however, the separation factor increases with an increasing of acetic acid concentration in the feed solution. As acetic acid concentration in the feed solution increases, the dissolution of acetic acid molecules into the membrane is weaken, which would decrease the swelling degree of membrane. Accordingly, free volume of the membrane gets smaller, leading to an enhancing in separation factor at the cost of permeation flux. Similar trends have been reported by other researchers.[42–44] This is a trade-off

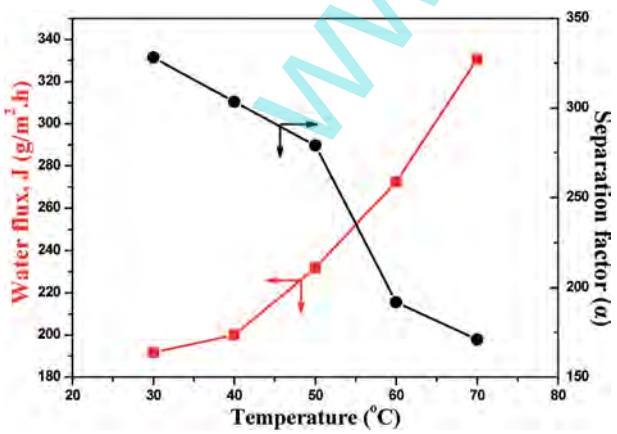

Fig. 10 Effect of temperature of feed on pervaporation performance of NH_2-MIL-125(Ti)/NaAlg-6 MMMs (90 wt% acetic acid in feed at 30 °C).

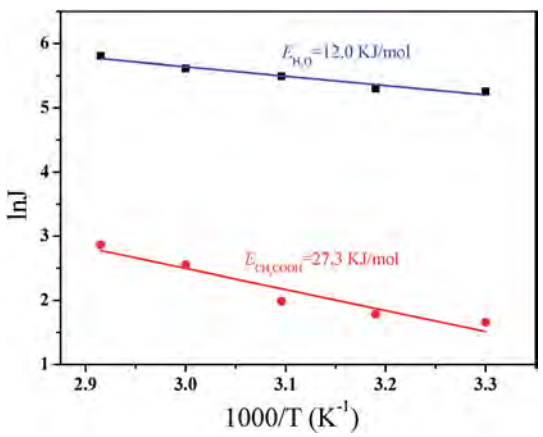

Fig. 11 Variation of ln J *vs.* $1/T$ for NH_2-MIL-125(Ti)/NaAlg-6 MMMs in pervaporation of 90 wt% acetic acid in feed.

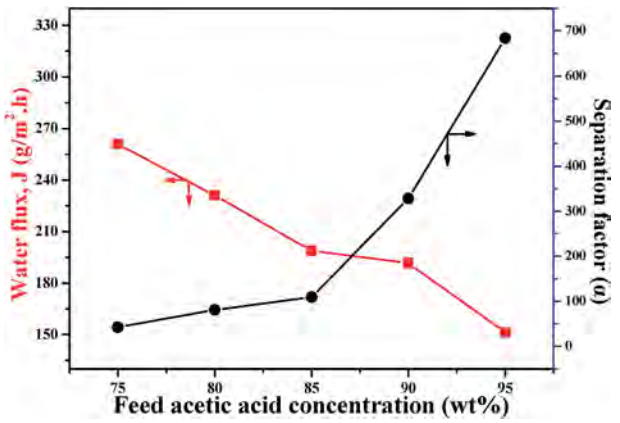

Fig. 12 Effect of acetic acid concentration on pervaporation performance of NH_2-MIL-125(Ti)/NaAlg-6 MMMs at 30 °C.

phenomenon and typically observed in pervaporation process. Moreover, at a higher acetic acid concentration, acetic acid molecules tend to form dimers with larger sizes, which leads to more difficulty for acetic acid molecules to diffuse through the membrane.[45]

3.3.4. Effect of feed flow rate on pervaporation performance. Effect of feed flow rate on the pervaporation performance of the as-prepared NH_2-MIL-125(Ti)/NaAlg-6 MMMs is presented in Fig. 13. It can be observed that water flux increases while separation factor decreases with an increasing of feed flow rate from 350 to 440 mL min^{-1}. With feed flow rate increasing, the turbulence of feed solution increases and the thickness of boundary layer decreases, thus results in a decreasing of mass transfer resistance in the boundary layer and a decreasing of concentration polarization on the upstream of membrane. As a result, higher feed flow rates can enhance total permeation flux, however, isn't beneficial for separation selectivity.

3.4. Comparison of the pervaporation performance of the NH_2-MIL-125(Ti)/NaAlg-6 MMMs with literature data

A comparison of the present pervaporation results with the published results is important to assess the superiority of the present membrane. The pervaporation data are compared in Table 2 with the available literature data. We found that the pervaporation performance of the NH_2-MIL-125(Ti)/NaAlg-6 MMMs in separation water/acetic acid mixtures is encouraging.

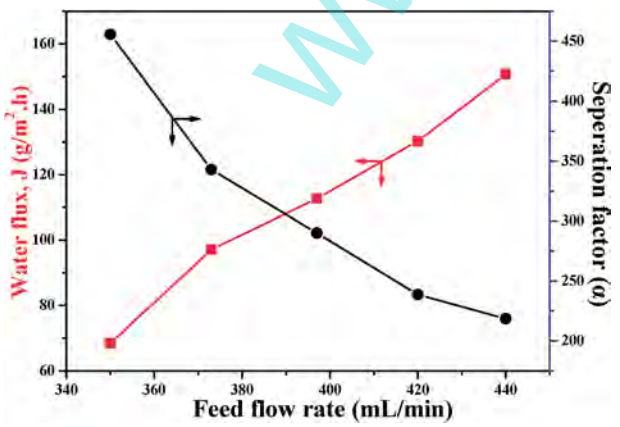

Fig. 13 Effect of feed flow rate on pervaporation performance of NH_2-MIL-125(Ti)/NaAlg-6 MMMs (90 wt% acetic acid in feed at 30 °C).

Table 2 Comparison of pervaporation performance of NH_2-MIL-125(Ti)/NaAlg MMMs with literature data at different operation condition in separation water/acetic acid mixtures[a]

Membranes	Water (wt%)	Temperature (°C)	Flux (g m^{-2} h)	Separation factor	Reference
STA-PVA-SPEK-C-GA	20	50	680	75	3
SPEK-C-GA	10	40	280	133	3
PVA/TEOS (0.5 wt%)	10	30	113	36	6
PVA/TEOS (1.0 wt%)	10	30	70	441	6
PVA/TEOS (1.5 wt%)	10	30	48	741	6
PVA/TEOS (2.0 wt%)	10	30	33	1116	6
Ca-Alg/MPPM	10	40	127	2078	42
NaAlg crosslinked with GA	10	40	154	15	46
NaAlg/PAN/PVA	10	50	94	18	47
NaAlg/PVA	15	40	44	46	47
SPBI	10	22	98	24 000	48
NaAlg/PVA/PEG	10	30	50	3591	49
PVA/PAA	10	25	300	6.60	50
PVA/PHC	10	25	140	7.90	50
PVA/PVP	10	25	800	2.40	50
PEC/PW_{11}	10	50	440	144	51
PVA-*g*-AN (52%) (PVA-2)	10	30	90	14.6	52
PVA-*g*-PAAm	20	35	56	3.9	53
ZSM-5 zeolite membranes	5	90	490	7.7	54
SPEK-C/PVA	10	50	492	59.3	55
NH2-MIL-125(Ti)/NaAlg-6 MMMs	10	30	196.7	328.1	This work

[a] MPPM: microporous polypropylene membrane; SPBI: sulfonated polybenzimidazole; PEG: polyethylene glycol; PEC: polyelectrolytes complex; PW_{11}: 11-phosphotungstic acid hydrate; AN: acrylonitrile.

4. Conclusion

In this work, we have studied the effect of incorporation of NH_2-MIL-125(Ti) nanoparticles on the separation performance of the NaAlg-based mixed matrix membranes for the separation of acetic acid and water mixtures. Characterization results revealed that NH_2-MIL-125(Ti) nanoparticles were well dispersed in the NaAlg matrix due to the good compatibility between NH_2-MIL-125(Ti) nanoparticles and NaAlg matrix. The pervaporation tests results demonstrated that the incorporating of appropriate amount of NH_2-MIL-125(Ti) nanoparticles into the NaAlg matrix could significantly enhance the pervaporation performance of NH_2-MIL-125(Ti)/NaAlg MMMs. The pervaporation performances of NH_2-MIL-125(Ti)/NaAlg-6 MMMs were

greatly influenced by feed temperature, feed acetic acid concentration and feed flow rate. The NH_2-MIL-125(Ti)/NaAlg-6 MMMs show a high separation factor of 328 and flux of 190.7 g m^{-2} h^{-1} for pervaporation dehydration of 90 wt% acetic acid aqueous. The results demonstrate that the NH_2-MIL-125(Ti)/NaAlg-6 MMMs can be expected as promising membranes for dehydration of organic solvent.

Acknowledgements

The authors would like to acknowledge the financial support of this work from National Natural Science Foundation of China (No. 21076174), Natural Science Foundation of Fujian (2012J06005 and 2014J01051). The authors also thank the anonymous referees for comments on this manuscript.

References

1 S. S. Kulkarni, S. M. Tembe and M. Y. Karidurgannavar, *J. Membr. Sci.*, 2006, **285**, 420.
2 S. B. Kuila and S. K. Ray, *Sep. Purif. Technol.*, 2011, **81**, 295.
3 S. K. Ray, S. B. Sawant, J. B. Joshi and V. G. Pangarkar, *J. Membr. Sci.*, 1998, **138**, 1.
4 J. H. Chen, Q. L. Liu, Y. Xiong, Q. G. Zhang and A. M. Zhu, *J. Membr. Sci.*, 2008, **325**, 184.
5 Y. C. Wang, C. L. Li and K. R. Lee, *J. Membr. Sci.*, 2002, **208**, 3.
6 M. Y. Kariduraganavar, S. S. Kulkarni and A. A. Kittur, *J. Membr. Sci.*, 2005, **246**, 83.
7 J. H. Chen, Q. L. Liu, A. M. Zhu, J. Fang and Q. G. Zhang, *J. Membr. Sci.*, 2008, **308**, 171.
8 X. Feng and R. Y. M. Huang, *Ind. Eng. Chem. Res.*, 1997, **36**, 1048.
9 Q. G. Zhang, G. L. Han, W. W. Hu, A. M. Zhu and Q. L. Liu, *Ind. Eng. Chem. Res.*, 2013, **52**, 7541.
10 L. M. Robeson, *J. Membr. Sci.*, 1991, **62**, 165.
11 L. M. Robeson, *J. Membr. Sci.*, 2008, **320**, 390.
12 A. C. Balazs, T. Emrick and T. P. Russell, *Science*, 2006, **314**, 1107.
13 T. Li, Y. C. Pan, K. V. Peinemann and Z. P. Lai, *J. Membr. Sci.*, 2013, **435**, 235.
14 T. S. Chung, L. Y. Jiang, Y. Li and S. Kulprathipanja, *Prog. Polym. Sci.*, 2007, **32**, 483.
15 A. A. Kittur, M. Y. Kariduraganavar, S. S. Kulkarni and M. I. Aralaguppi, *J. Appl. Polym. Sci.*, 2005, **96**, 1377.
16 H. K. Chae, D. Y. Siberio-Pérez, J. Kim, Y. Go, M. Eddaoudi, A. J. Matzger, M. O'keeffe and O. M. Yaghi, *Nature*, 2004, **427**, 523.
17 S. Basu, A. L. Khan, A. Cano-Odena, C. Liu and I. F. J. Vankelecom, *Chem. Soc. Rev.*, 2010, **39**, 750.
18 H. B. T. Jeazet, C. Staudt and C. Janiak, *Dalton Trans.*, 2012, 14003.
19 T. X. Yang and T. S. Chung, *J. Mater. Chem. A*, 2013, **19**, 6081.
20 Q. Song, S. K. Nataraj, M. V. Roussenova, J. C. Tan, D. J. Hughes, W. Li, P. Bourgoin, M. A. Alam, A. K. Cheetham, S. A. Al-Muhtaseb and E. Sivaniah, *Energy Environ. Sci.*, 2012, **5**, 8359.
21 H. Q. Ren, J. Y. Jin, J. Hu and H. L. Liu, *Ind. Eng. Chem. Res.*, 2012, **51**, 10156.
22 T. H. Bae, J. S. Lee, W. L. Qiu, W. J. Koros, C. W. Jones and S. Nair, *Angew. Chem., Int. Ed.*, 2010, **49**, 9863.
23 X. L. Liu, Y. S. Li, G. Q. Zhu, Y. J. Ban, L. Y. Xu and W. S. Yang, *Angew. Chem., Int. Ed.*, 2011, **50**, 1.
24 X. Liu, H. Jin, Y. Li, H. Bux, Z. Hu, Y. Ban and W. Yang, *J. Membr. Sci.*, 2013, **428**, 498.
25 C. H. Kang, Y. F. Lin, Y. S. Huang, K. L. Tung, K. S. Chang, J. T. Chen, W. S. Hung, K. R. Lee and J. Y. Lai, *J. Membr. Sci.*, 2013, **438**, 105.
26 S. Sorribas, A. Kudasheva, E. Almendro, B. Zornoza, Ó. de la Iglesia, C. Téllez and J. Coronas, *Chem. Eng. Sci.*, 2015, **124**, 37.
27 D. Hua, Y. K. Ong, Y. Wang, T. Yang and T. S. Chung, *J. Membr. Sci.*, 2014, **453**, 155.
28 N. D. McNamara, G. T. Neumann, E. T. Masko, J. A. Urban and J. C. Hicks, *J. Catal.*, 2013, **305**, 217.
29 S. N. Kim, J. Kim, H. Y. Kim, H. Y. Cho and W. S. Ahn, *Catal. Today*, 2013, **204**, 85.
30 F. Jeremias, V. Lozan, S. K. Henninger and C. Janiak, *Dalton Trans.*, 2013, 15967.
31 P. Luis, J. Degrève and B. V. Bruggen, *J. Membr. Sci.*, 2013, **429**, 1.
32 S. G. Adoor, S. D. Bhat, D. D. Dionysiou, M. N. Nadagouda and T. M. Aminabhavi, *RSC Adv.*, 2014, **4**, 52571.
33 C. Zlotea, D. Phanon, M. Mazaj, D. Heurtaux, V. Guillerm, C. Serre, P. Horcajada, T. Devic, E. Magnier, F. Cuevas, G. Férey, P. L. Llewellyn and M. Latroche, *Dalton Trans.*, 2011, 4879.
34 Y. Li, L. H. Wee, J. A. Martens and I. F. J. Vankelecom, *J. Mater. Chem. A*, 2014, **2**, 10034.
35 S. N. Yu, F. S. Pan, S. Yang, H. Ding, Z. Y. Jiang, B. Y. Wang, Z. X. Li and X. Z. Cao, *Chem. Eng. Sci.*, 2015, **135**, 479.
36 D. P. Suhas, A. V. Raghu, H. M. Jeong and T. M. Aminabhavi, *RSC Adv.*, 2013, **3**, 17120.
37 S. Panahian, A. Raisi and A. Aroujalian, *Desalination*, 2015, **355**, 45.
38 S. N. Liu, G. P. Liu, X. H. Zhao and W. Q. Jin, *J. Membr. Sci.*, 2013, **446**, 181.
39 T. M. Aminabhavi, R. S. Khinnavar, S. B. Harogoppad, U. S. Aithal, Q. T. Nguyen and K. C. Hansen, *J. Macromol. Sci., Polym. Rev.*, 1994, **34**, 139.
40 X. Feng and R. Y. M. Huang, *J. Membr. Sci.*, 1996, **118**, 127.
41 V. T. Magalad, G. S. Gokavi, K. V. S. N. Raju and T. M. Aminabhavi, *J. Membr. Sci.*, 2010, **354**, 150.
42 W. Zhang, Y. X. Xu, Z. j. Yu, S. Lu and X. P. Wang, *J. Membr. Sci.*, 2014, **451**, 135.
43 S. P. Dharupaneedi, R. V. Anjanapura, J. M. Han and T. M. Aminabhavi, *Ind. Eng. Chem. Res.*, 2014, **53**, 14474.
44 Z. Huang, Y. Shi, R. Wen, Y. H. Guo, J. F. Su and T. Matsuura, *Sep. Purif. Technol.*, 2006, **51**, 126.
45 G. Li, E. Kikuchi and M. Matsukata, *J. Membr. Sci.*, 2003, **218**, 185.
46 S. B. Teli, G. S. Gokavi, M. Sairam and T. M. Aminabhavi, *Sep. Purif. Technol.*, 2007, **54**, 178.
47 X. N. Wang, *J. Membr. Sci.*, 2000, **170**, 71.

48 Y. Wang, T. S. Chung and M. Gruender, *J. Membr. Sci.*, 2012, **415**, 486.
49 U. S. Toti and T. M. Aminabhavi, *J. Membr. Sci.*, 2004, **228**, 199.
50 A. Rudin, *The Elements of Polymer Science and Engineering*, New York, 1982, Ch. 3, pp. 102.
51 J. H. Chen, J. Z. Zheng, Q. L. Liu, H. X. Guo, W. Weng and S. X. Li, *J. Membr. Sci.*, 2013, **429**, 206.
52 N. Alghezawi, O. Sanlı, L. Aras and G. Asman, *Chem. Eng. Process.*, 2005, **44**, 51.
53 G. H. Koops, J. A. M. Nolten, M. H. V. Mulder and G. A. Smolders, *J. Membr. Sci.*, 1993, **81**, 57.
54 W. G. Sun, X. W. Wang, J. H. Yang, J. M. Lu, H. L. Han, Y. Zhang and J. Q. Wang, *J. Membr. Sci.*, 2009, **335**, 83.
55 J. H. Chen, Q. L. Liu, A. M. Zhu and Q. G. Zhang, *J. Membr. Sci.*, 2008, **320**, 416.